

# Semaphorin3A Promotes the Development of Nickel Allergy

**Lipei Liu**

Tokushima University, Graduate School of Biomedical Sciences

**Megumi Watanabe** (✉ [megwat@tokushima-u.ac.jp](mailto:megwat@tokushima-u.ac.jp))

Tokushima University, Graduate School of Biomedical Sciences

**Norikazu Minami**

Tokushima University, Graduate School of Biomedical Sciences

**Mohammad Yunizar**

Institute of Biomedical Sciences, Tokushima University

**Tetsuo Ichikawa**

Institute of Biomedical Sciences, Tokushima University <https://orcid.org/0000-0003-0950-9957>

---

## Article

**Keywords:** Semaphorin3A, Nickel Allergy, Metal allergy, keratinocytes

**Posted Date:** June 21st, 2021

**DOI:** <https://doi.org/10.21203/rs.3.rs-598449/v1>

**License:**   This work is licensed under a Creative Commons Attribution 4.0 International License.

[Read Full License](#)

---

**Version of Record:** A version of this preprint was published at Communications Biology on July 7th, 2022.  
See the published version at <https://doi.org/10.1038/s42003-022-03641-0>.

# 1 **Semaphorin3A Promotes the Development of Nickel Allergy**

2

## 3 **Abstract**

4 Metal allergy is one of the typical immune disorders encountered during the application of  
5 dental/medical materials and has a highly complex pathogenic mechanism. Semaphorin 3A (Sema3A),  
6 a member of the semaphorin family, is reported to be involved in various immune disorders. However,  
7 its role in metal allergy has not been clarified yet. Herein, we show that Sema3A promoted nickel (Ni)  
8 allergy by mediating tumor necrosis factor-alpha (TNF- $\alpha$ ) production and mitogen-activated protein  
9 kinase (MAPK) activation in keratinocytes. Sema3A was upregulated in NiCl<sub>2</sub>-stimulated mouse  
10 keratinocytes and in Ni allergy-induced mouse ear tissue. TNF- $\alpha$  production and MAPK activation  
11 were altered when Sema3A was suppressed in keratinocytes. The specific deletion of Sema3A in  
12 keratinocytes alleviated Ni allergy and regulated the macrophage polarization towards an anti-  
13 inflammatory direction. Our results demonstrate that Sema3A promotes the development of metal  
14 allergy and should be explored as a potential target for the prevention and treatment of metal allergy.

15

## 16 **Introduction**

17 Metal allergy, one of the typical disorders of the immune system, is a major challenge in the  
18 application of dental/medical materials<sup>1</sup>. It is estimated that up to 17% of women and 3% of men are  
19 allergic to Ni and that 1-2% of individuals are allergic to cobalt, chromium, or both<sup>2</sup>. Metal allergy not  
20 only causes treatment failure but also affects the skin throughout the body; it has been reported to be  
21 associated with lichen planus lesions and palmoplantar pustulosis<sup>3, 4, 5</sup>. An acidic diet, decomposition  
22 of food residues, and bacterial metabolism in the oral cavity result in chemical corrosion of metal  
23 materials<sup>6</sup>. Corroded and ionized metals tend to cause metal allergy; however, the mechanism is highly  
24 complex and many puzzles remain to be solved.

25 It takes repeated or prolonged exposure to develop a metal allergy. Metal ions released from various  
26 alloys that come in contact with the skin could activate epithelial cells, such as keratinocytes, to  
27 produce cytokines or chemokines, as well as activate antigen-presenting cells (APCs), such as  
28 dendritic cells (DCs) and Langerhans cells. After APCs present antigens to naïve T cells in the draining  
29 lymph nodes, the differentiated effector T cells migrate to the peripheral tissues and lead to allergic  
30 reactions<sup>7</sup>.

31 Ni, among various metals, is the most common allergen that causes metal allergy<sup>8</sup>. We successfully  
32 built a Ni allergy mouse model in our previous study<sup>9, 10, 11</sup>. Using this model, we demonstrated that

33 the activation of DCs through p38 MAPK/MKK6 is important for the development of Ni allergy in  
34 mice<sup>9</sup> and that the thymic stromal lymphopoietin (TSLP)/TSLP receptor-mediated interaction between  
35 epithelial and immune cells could trigger Ni allergy<sup>10</sup>. We have also demonstrated that semaphorin 7A,  
36 a member of the semaphorin family, enhances inflammation during the effector phase of Ni allergy<sup>11</sup>.

37 Semaphorins are a type of secreted and membrane proteins that were initially recognized as axon  
38 guide molecules. Accumulating evidence suggests that semaphorins are involved in the pathogenesis  
39 of several immune disorders<sup>12</sup>. Sema3A, a member of the semaphorin family, is known to function as  
40 an effective immunomodulator in immune cell migration and regulation<sup>13, 14, 15, 16, 17</sup>. Sema3A  
41 downregulates T cell proliferation via the neuropilin-1(Nrp1)-plexin-A4 receptor complex<sup>17</sup> and  
42 increases cytokine production in response to toll like receptor (TLR) agonists or bacterial sepsis in  
43 mice<sup>18</sup>. Sema3A is also involved in DC transmigration from the periphery to draining lymph nodes<sup>17</sup>.  
44 Besides, Sema3A has been reported to be associated with various immune diseases, such as rheumatoid  
45 arthritis and systemic lupus erythematosus<sup>19</sup>. It also controls the inflammatory responses in allergic  
46 conjunctivitis and allergic rhinitis<sup>20, 21</sup>. Recent studies have suggested that Sema3A could interrupt the  
47 itch-scratch cycle by inhibiting the extension and sprouting of C-fiber in the epidermis, thereby  
48 alleviating the skin lesions and scratching behavior of NC/Nga mice, a model of atopic dermatitis (AD),

49 in a dose-dependent manner<sup>22, 23</sup>. Furthermore, Sema3A has been shown to inhibit the migration of  
50 CD4<sup>+</sup> T cells to inflammatory sites<sup>22</sup>. Considering its role as a potent inhibitor of neurite outgrowth of  
51 sensory neurons and inflammatory cell infiltration, Sema3A has been extensively studied for its  
52 potential in the treatment of refractory itching skin diseases that exogenous application of Sema3A  
53 improves the pathophysiology of AD and psoriasis<sup>24</sup>; however, the association between Sema3A and  
54 metal allergy has not yet been reported.

55 To better clarify the molecular mechanism underlying metal allergy, in this study, we used an Ni  
56 allergy mouse model to study the role of Sema3A in Ni allergy. We speculated that Sema3A, being a  
57 secretory protein, might function like cytokines or chemokines and may play a crucial role in both  
58 intercellular and intracellular communication, thereby influencing the process of metal allergy  
59 development and becoming a potential target for the investigation and treatment of metal allergy.

60

## 61 **Results**

### 62 **Sema3A is upregulated in keratinocytes when stimulated with NiCl<sub>2</sub>**

63 The epidermis, which is the outermost layer of the skin, is the first barrier against antigen invasion  
64 and plays vital roles in the development of metal allergy<sup>25</sup>. We aimed to determine whether there is

65 any interaction between Sema3A and keratinocytes, which constitute 90% of the cells of the epidermis,  
66 thereby contributing to metal allergy. To investigate Sema3A expression in keratinocytes, we  
67 stimulated the Pam2.12 keratinocyte cell line with NiCl<sub>2</sub> for different durations. The Sema3A mRNA  
68 expression was upregulated in keratinocytes exposed to NiCl<sub>2</sub>-stimulation over time, although there  
69 was no significant difference (Fig. 1a). The staining of keratinocytes with Sema3A antibody showed  
70 brightly positive cytoplasmic secretory granules which filled the entire cell cytoplasm. These positive  
71 granules were observed to be more strongly expressed on keratinocytes 24 and 48 h after NiCl<sub>2</sub>  
72 stimulation compared to those in the control group (Fig. 1b). The expression of Sema3A protein was  
73 also upregulated and reached a peak 12 h after NiCl<sub>2</sub> stimulation by Western blotting (Fig. 1c). 72 h  
74 after NiCl<sub>2</sub> stimulation, the significantly increased production of Sema3A in the culture medium of  
75 Pam2.12 was confirmed by ELISA (Fig. 1d).

76

### 77 **Sema3A knockdown in keratinocytes alters MAPK activation and TNF- $\alpha$ expression**

78 To evaluate the functional role of Sema3A in keratinocytes, Pam2.12 cells were transfected with  
79 Sema3A siRNA. Without the stimulation of NiCl<sub>2</sub>, the expression of TNF- $\alpha$ , a known inflammatory  
80 cytokine produced by keratinocytes<sup>7</sup>, showed no significant difference among groups. However, when

81 cells were stimulated with NiCl<sub>2</sub>, the NiCl<sub>2</sub>-stimulated control and mock group showed higher TNF- $\alpha$   
82 expression than the non-stimulated groups. The expression of TNF- $\alpha$  in the Sema3A-silenced group  
83 was significantly inhibited compared to that in the mock group 24 h after NiCl<sub>2</sub> stimulation (p=0.026  
84 and 0.0014 respectively) (Fig. 2a, b). The cells, 48 h post-siRNA transfection, seemed to recover and  
85 exhibited less efficient suppression of TNF- $\alpha$  mRNA than that at 24 h post-siRNA transfection (Fig.  
86 2a). We then checked the expression of TSLP, which is considered a master switch for allergic  
87 inflammation and a downstream molecule of TNF- $\alpha$ <sup>26</sup>, in NiCl<sub>2</sub>-stimulated Pam2.12. The protein  
88 expression of TSLP was activated in NiCl<sub>2</sub>-stimulated Pam2.12 and showed a peak 12 h after  
89 stimulation (Supplementary Figure 1), consistent with the result of Ashrin in that TSLP production  
90 increased in the epidermal keratinocyte COCA cell line stimulated with NiCl<sub>2</sub><sup>10</sup>. We also assessed the  
91 MAPK activation in Pam2.12. In Sema3A-silenced Pam2.12, the activation of p38 was significantly  
92 inhibited 24 h after NiCl<sub>2</sub> stimulation compared to that in the control 1 (p=0.018). The suppression  
93 effect of siRNA seemed to recover 48 h after stimulation but the protein expression of p38 was still  
94 lower than that in the control group (Fig. 2c). These results suggest that Sema3A may play a role in  
95 triggering or regulating the process of Ni allergy through mediating p38 kinase activation and TNF- $\alpha$   
96 expression produced by keratinocytes.

97

98 **Sema3A is enhanced in Ni allergy-induced mouse ear tissue**

99 To investigate Sema3A expression *in vivo*, we induced Ni allergy in mice as described previously<sup>9</sup>  
100 (Fig. 3a). After 48 h of Ni re-challenge, delayed-type hypersensitivity (DTH) reaction, characterized  
101 by severe swelling and redness in the ear tissue, was confirmed in the allergy-induced group (Fig. 3b).  
102 Hematoxylin and eosin (H&E) staining showed increased thickness and more infiltrated cells in the  
103 allergy-induced ear tissue (Fig. 3c). Ear thickness was significantly increased 24, 48, and 72 h after  
104 NiCl<sub>2</sub> injection compared to that in the control group (Fig. 3e). Sema3A expression was found to be  
105 mainly located in the epidermis layer and expressed more strongly than that in the control (Fig. 3d).  
106 Consistently, the western blotting results of Sema3A showed significantly stronger expression in the  
107 Ni allergy group than in the control (p=0.000024) (Fig. 3f). We also investigated some inflammatory  
108 cytokines and chemokines associated with skin inflammation. The upregulation of IL-17, L-23,  
109 CCL20, and CXCL1 mRNA was observed in Ni allergy-induced mouse ear tissues (Fig. 3g). Since  
110 Sema3A expression is strongly enhanced in Ni allergy-induced mouse ear tissue than in the control,  
111 we speculate that Sema3A may be positively correlated with the development of Ni allergy.

112

113 **The number of monocytes, macrophages, and DCs increases in Ni allergy-induced mouse ear**  
114 **tissue**

115 Results of flow cytometry showed that the number of CD11b<sup>+</sup> cells increased markedly in the Ni  
116 allergy-induced groups (Fig. 4a, d). Among them, the number of CD11b<sup>+</sup>CD115<sup>+</sup> monocytes increased  
117 in the Ni allergy-induced ear tissue compared to that in the control group (Fig. 4a, b). Following  
118 immunofluorescence staining of frozen sections, an increased number of monocytes was observed in  
119 the Ni allergy-induced ear tissue (Fig. 4c). Similarly, an increase in the number of CD11b<sup>+</sup>F4/80<sup>+</sup>  
120 macrophages was observed in the Ni allergy-induced group compared to that in the control group  
121 (p=0.006) (Fig. 4d-f). The number of CD11c<sup>+</sup>MHC class II<sup>+</sup> DCs was found to be increased in the Ni  
122 allergy-induced group, and the immunofluorescence staining of epidermal sheet showed coincident  
123 results (p=0.002) (Fig. 4g-i). These results indicate the involvement of monocytes, macrophages, and  
124 DCs in the development of Ni allergy.

125

126 **Sema3A-specific deletion in keratinocytes reduces Ni allergy**

127 Sema3A is reported to mainly localize in the keratin14-positive keratinocytes in the stratum basale  
128 of the human epidermis<sup>27</sup>. Therefore, to investigate the role of Sema3A in Ni allergy *in vivo*, we crossed

129 *Sema3A*<sup>fl/fl</sup> mice with keratin5 (K5)-Cre mice using a cre/loxp system to knockout *Sema3A* in K5,  
130 which is a similar protein and partner of keratin14. The DTH reaction was confirmed in *Sema3A*<sup>fl/fl</sup>  
131 mice, similar to that in C57BL/6J mice; therefore, we used *Sema3A*<sup>fl/fl</sup> mice as a control group in the  
132 confirmation of Ni allergy development in *Sema3A* conditional knockout (cKO) mice. The results  
133 showed that the development of Ni allergy and inflammatory reactions was alleviated in *Sema3A* cKO  
134 mice compared to that in the control mice (Fig. 5a). After 24 h Ni elicitation, the ear thickness of the  
135 control mice was significantly increased in the Ni allergy-induced ear tissue than in the control  
136 ( $p=0.000015$ ), while the ear thickness of *Sema3A* cKO mice just increased slightly, and not to the  
137 degree of the control group (Fig. 5b). After 48 h, the ears of the control mouse remained to be red and  
138 swollen; however, the ears of *Sema3A* cKO mice almost recovered to normal (Fig. 5a, b). The ratio of  
139 Ni allergy-induced ear thickness to the control ear thickness, which represents the degree of thickening  
140 of ears, was significantly lower in the *Sema3A* cKO group ( $p=0.018$  and  $0.001$  respectively) than in  
141 the control group 24 h and 48 h post-Ni re-challenge (Fig. 5b). In other words, when inducing Ni  
142 allergy, the ear swelling in *Sema3A* cKO mice was less severe than that in the control mice. In the  
143 H&E staining of Ni allergy-induced ear tissue of *Sema3A* cKO mice, less severe edema and fewer  
144 infiltrated inflammatory cells were observed than in the control mice (Fig. 5c). To determine the genes,

145 cytokines, and chemokines associated with Sema3A deletion in keratinocytes, we further investigated  
146 the expression levels of TNF- $\alpha$ , IL-1 $\beta$ , IL-23, and CXCL1, which were found to be significantly  
147 enhanced in the Ni allergy-induced control mouse ear tissue but blunted in the Sema3A cKO group.  
148 The upregulation of CCL20 seemed to be unaffected with the deletion of Sema3A (Fig. 5d). These  
149 results indicate that Sema3A probably promotes the development of Ni allergy.

150

#### 151 **Sema3A-specific deletion in keratinocytes increases M2/M1 macrophage polarization**

152 To examine the change in immune cell profiles during Ni allergy development in Sema3A cKO mice,  
153 flow cytometry was performed. An increased number of CD11b<sup>+</sup>F4/80<sup>+</sup> macrophages was detected in  
154 both control and Sema3A cKO Ni allergy-induced groups, and there was no apparent difference  
155 between them (Fig. 6a). CD206 was used to further determine M1 and M2 macrophages. The analysis  
156 revealed that the proportion of CD206<sup>+</sup>CD11b<sup>+</sup>F4/80<sup>+</sup> M2-like macrophages increased significantly in  
157 the Sema3A cKO Ni allergy-induced group (Fig. 6a, b). The ratio of CD206<sup>+</sup>CD11b<sup>+</sup>F4/80<sup>+</sup>M2-like  
158 macrophages to CD206<sup>-</sup>CD11b<sup>+</sup>F4/80<sup>+</sup> M1-like macrophages was significantly increased in the  
159 Sema3A cKO Ni allergy-induced group compared to that in the control group (p=0.014) (Fig. 6c). This  
160 result indicates that the alleviated Ni allergy in Sema3A cKO mice might be related to the polarization

161 of macrophage towards the M2 phenotype, which produces anti-inflammatory cytokines that  
162 contribute to tissue healing.

163

## 164 **Discussion**

165     Sema3A is the member of the semaphorin family known to function as an axonal repulsion factor  
166 through interaction with the plexinA/Nrp1 receptor<sup>12</sup>. The significance of sema3A in regulating  
167 immune-mediated inflammation has been widely reported, as an example, the expression level of  
168 Sema3A in the epidermis of patients with AD and psoriasis was remarkably decreased compared to  
169 that in healthy volunteers<sup>28</sup> and in the epidermis of AD patients, epidermal hyperinnervation and high  
170 levels of nerve growth factor (NGF) were observed<sup>29</sup>. Since Sema3A is known to inhibit the  
171 intraepidermal extension of peripheral nerve and has been reported to abolish the growth promoting  
172 effect of NGF on sensory afferents in adult rat spinal cord and mouse embryonic neurons<sup>30, 31, 32</sup>, the  
173 epidermal innervation in AD and psoriasis is likely to be regulated by a balance of NGF and Sema3A,  
174 and the decreased Sema3A in the epidermis of these patients could result from increased NGF. In our  
175 study, the expression of Sema3A was increased in the inflammatory site of the skin of metal allergy  
176 mouse models, suggesting that Sema3A may be involved in the pathogenesis of both diseases through

177 different mechanisms. Previous studies have demonstrated that activated keratinocytes can release  
178 certain proinflammatory cytokines such as IL-1 $\beta$  and TNF- $\alpha$ , TSLP, and chemokines in response to  
179 pathogens, injury and wound healing as well as cancers<sup>7, 33, 34, 35</sup>. In addition, recent studies on the  
180 effect of Sema3A on immune response have reported its association with TNF- $\alpha$  and MAPK pathway.  
181 In our results, both TNF- $\alpha$  and p38 kinase expressions were inhibited when Sema3A was suppressed  
182 in keratinocytes. In previous studies, significantly decreased TNF- $\alpha$  expression in microglial cells in  
183 response to TLR4 stimulation was observed with the knockdown of the receptor of PlexinA1, which  
184 is a receptor of Sema3A<sup>36, 37</sup>. These results reflect the possibility that the production of TNF- $\alpha$  on  
185 keratinocytes stimulated with NiCl<sub>2</sub> depends on Sema3A secretion.

186 On the other hand, keratinocytes stimulated with NiCl<sub>2</sub> resulted in activation of p38, and inhibition  
187 of Sema3A with siRNA inhibited activation of p38. It is known that p38 promotes the upregulation of  
188 IL-1 $\beta$  and TNF- $\alpha$ , which are strongly involved in skin inflammation<sup>38, 39</sup>. In addition, studies using  
189 itch-deficient (Itch<sup>-/-</sup>) mice showed enhancement of phosphorylation of p38 $\alpha$  in skin lesions, and  
190 proinflammatory cytokines such as TNF- $\alpha$  and IL-1 $\beta$  were increased in the skin of Itch<sup>-/-</sup> mice.  
191 Moreover, that inhibition of p38 significantly suppresses inflammation in the skin of Itch<sup>-/-</sup> mice<sup>40</sup>.  
192 Therefore, our results suggest that inhibition of Sema3A expression may have suppressed TNF- $\alpha$

193 secretion by inhibiting p38 in keratinocytes.

194 Keratinocytes, which make up the majority of epidermal cells, are the first cells to have access to  
195 metal ions coming from the outside. When keratinocytes come in contact with metal ions, they secrete  
196 abundant Sema3A and TNF- $\alpha$ . TNF- $\alpha$  has been reported to promote tissue repair and enhance  
197 keratinocyte motility and attachment<sup>41, 42</sup>. It also regulates innate immunity and inflammation by  
198 inducing chemokines that attract neutrophils, macrophages, and skin-specific memory T-cells<sup>43</sup>. In our  
199 study, we observed an increase in the number of monocytes and macrophages in the Ni allergy ear  
200 tissue by flow cytometry analysis, which implicates TNF- $\alpha$  produced by keratinocytes in the  
201 pathogenesis of Ni allergy by attracting the immune cells via chemokines such as CXCL1 to initiate  
202 the process of inflammation. CXCL1 is known as keratinocyte-derived chemokines and is expressed  
203 on macrophages, neutrophils, and epithelial cells and activates the ERK pathway during the  
204 inflammatory response and contributes to the inflammatory process<sup>44</sup>. In our study, when CXCL1  
205 expression was upregulated in allergic skin and downregulated when Sema3A was inhibited in the ear  
206 skin using siRNA or in the cKO mice at the onset of allergy, CXCL1 was reduced and TNF- $\alpha$   
207 expression was also suppressed. Altogether, Sema3A promotes the secretion of TNF- $\alpha$  and attracts  
208 immune cells via CXCL1, which is expressed as a result, and induces local allergic reactions.

209 In recent years, polarized macrophages have acquired significant attention. M1 macrophages are  
210 reported to promote the process of inflammation, while M2 macrophages suppress inflammation<sup>45</sup>.  
211 Therefore, the balance of M1/M2 macrophage activity plays a significant role in physiology and  
212 pathology. In our study, Sema3A cKO mice were protected against Ni allergy. Furthermore, a high  
213 M2/M1 ratio, which represents the anti-inflammatory responses, was observed in the Sema3A cKO  
214 allergy-induced group, while blunted upregulation of inflammatory cytokines/chemokines TNF- $\alpha$ , IL-  
215 1 $\beta$ , IL-23, and CXCL1 was detected. It has been widely accepted that M1 macrophages could be  
216 typically induced by TNF- $\alpha$ <sup>46, 47</sup>, and there are reports that reduction in TNF- $\alpha$  mRNA could result in  
217 enhanced M2 mRNA expression<sup>48</sup>, TNF- $\alpha$  deletion could inhibit M1 macrophage polarization<sup>49</sup>.  
218 Therefore, we speculate that the increased M2/M1 ratio in Ni allergy-induced Sema3A cKO mice in  
219 our study might be caused by the reduced TNF- $\alpha$  production in keratinocytes due to Sema3A-specific  
220 deletion in keratinocytes. The production of cytokine/chemokines produced by M1 macrophages, such  
221 as TNF- $\alpha$ , IL-23, and CXCL1, was hindered, thus reducing the inflammation and impeding the process  
222 of Ni allergy. In some studies, recombinant Sema3A protein was reported to affect the proinflammatory  
223 state of macrophages and increase the expression of M1-markers, such as inducible nitric oxide  
224 synthase (iNOS) and cyclooxygenase-2 (COX-2), with the stimulation of lipopolysaccharide (LPS)<sup>50</sup>.

225 Therefore, there is also a possibility that the deletion of Sema3A directly affects the polarization of  
226 M1 macrophages.

227 Intradermal injection or ointment allocation of Sema3A were found to inhibit scratching behavior  
228 to improve AD-like symptoms compared to controls. Moreover, the nerve fiber number in epidermis,  
229 inflammatory cell infiltration, and the cytokine production were reduced in Sema3A-treated skin  
230 lesion<sup>22,23</sup>. Decreased Sema3A concentration may lead to the occurrence or enhancement of itching in  
231 AD patients and NC/Nga mice<sup>51,52</sup>. In the studies above, exogenous Sema3A was applied to the lesions  
232 during inflammation, which is different from our study as we blocked endogenous Sema3A before the  
233 initiation of inflammation, which reduced the Ni allergy reaction successfully in the initial phase. It is  
234 presumed that exogenous Sema3A, in addition to inhibiting the elongation of epidermal nerve fibers,  
235 could downregulate endogenous Sema3A mRNA expression in keratinocytes through autocrine signal  
236 transduction, and finally inhibit the occurrence of inflammation by mediating the expression of TNF-  
237  $\alpha$ . Further confirmation, such as quantitative RT-PCR or western blotting of endogenous Sema3A  
238 mRNA expression upon exogenous Sema3A, is required in this regard.

239 In conclusion, through this study, we clarified that Sema3A could promote the development process  
240 of Ni allergy by mediating the activation of MAPK and the production of TNF- $\alpha$ . The specific deletion

241 of *Sema3A* in keratinocytes results in reduced *TNF- $\alpha$*  expression, which regulates the macrophage  
242 M1:M2 balance towards an anti-inflammatory direction, resulting in alleviated Ni allergy. It is  
243 conceivable that *Sema3A* has the potential to be further developed to provide new ideas and therapeutic  
244 targets for metal allergy.

245

## 246 **Methods**

### 247 Mice

248 Female C57BL/6J mice (8-week-old) were purchased from Charles River Laboratories, Inc.  
249 (Kanagawa, Japan). K5-cre<sup>53</sup> mice (STOCK-Tg(K5-Cre) Jt) were obtained from CARD R-BASE,  
250 Kumamoto University. K5-Cre-specificity was determined following the PCR protocol described  
251 previously<sup>54</sup>. *Sema3A*<sup>fl/fl</sup> mice (ICR.Cg-*Sema3a*<sup><tm1.2Tyag></sup>/*TyagRbrc*, RBRC01106) were provided  
252 by RIKEN BRC through the National BioResource Project of the MEXT/AMED, Japan. The  
253 genotyping of *Sema3A*<sup>fl/fl</sup>-specificity was performed according to the previous study<sup>55</sup>. *Sema3A*<sup>fl/fl</sup>  
254 conditional mice were crossed with K5-Cre mice to generate *Sema3A* cKO mice. Wild-type mice of  
255 the same genetic background strains were used as control animals. All mice used were aged 6-8 weeks.  
256 All mice were maintained under specific pathogen-free conditions and fed with autoclaved diet and

257 water in the animal facilities at Tokushima University, they were treated in accordance with the  
258 National Institutes of Health Guide for the Care and Use of Laboratory Animals. All experimental  
259 procedures were approved by IACUC (No. T2019-51) and Institute for Genome Research (No.30-46)  
260 of Tokushima University.

261

## 262 Reagents

263 Nickel(II) Chloride was obtained from Wako Pure Chemical Corporation. Freund's incomplete  
264 adjuvant (IFA) and complete adjuvant (CFA) were from MP Biomedicals. The primary antibodies  
265 specific for Sema3A were from Bioss Antibodies (for Western blotting) and Abcam (for  
266 immunohistochemistry/immunocytochemistry), respectively. Antibodies specific for phospho-p38  
267 (Thr180/Tyr182) and p38 were obtained from Cell Signaling Technology. Antibody specific for mouse  
268 TSLP was from Abcam. Rabbit antibody to GAPDH was obtained from Osenses. Alexa Fluor 488  
269 anti-mouse CD11c, Alexa Fluor 488 anti-mouse CD11b, PE anti-mouse CD115, PE anti-mouse F4/80,  
270 PE anti-mouse I-A/I-E and Alexa Fluor 647 anti-mouse CD206 (MMR) were purchased from  
271 BioLegend. Horseradish peroxidase (HRP)-conjugated anti-rabbit secondary antibody were obtained  
272 from Cell Signaling. Anti-rabbit Alexa Fluor 488 secondary antibody was from Abcam.

273

## 274 Induction of Ni Allergy

275 Ni allergy was induced on mouse ears as described previously<sup>9, 10, 11</sup>. In brief, 25µl 1mM NiCl<sub>2</sub> with  
276 25µl IFA was intraperitoneally injected to mice for initial immunization. After two weeks, 10µl 0.2mM  
277 NiCl<sub>2</sub> with 10µl CFA was intradermally injected into the ear skin as a second challenge. For negative  
278 control, PBS with CFA was injected. 48 h later, DTH reaction was observed and confirmed by  
279 measuring the ear thickness of mice.

280

## 281 Histology and immunofluorescence microscopy

282 Frozen sections (4-8µm) were stained with H&E. Sections for immunofluorescence staining were  
283 fixed with pre-cooled acetone (4 °C) for 10 minutes. After this, the slides were rinsed with PBS and  
284 blocked with 5% goat serum for 30 minutes. A 1:300 dilution of primary antibodies or fluorescently-  
285 conjugated antibodies was applied to the sections and incubated in a dark humidified chamber  
286 overnight at 4°C, subsequently followed by incubation with anti-rabbit Alexa 488 Fluor secondary  
287 antibody at room temperature for 1 h. The nuclei were stained with DAPI solution (0.1 µg/ml; Cell  
288 Signaling Technology, Danvers, MA, USA). Immunofluorescence images were captured using

289 Keyence all-in-one fluorescence-microscope BZ-X800 (magnification, ×200; ×400; ×1000;  
290 KEYENCE CORPORATION, Tokyo, Japan).

291

292 Epidermal sheet preparation

293 Epidermal sheets were prepared using a modification of previously-reported method<sup>56, 57</sup>. In brief,  
294 the ears were peeled into halves and put dermis-side down floating on a dish of cold ammonium  
295 thiocyanate. After incubated 13 minutes at 37 °C, the epidermal sheets were peeled with small tweezers.  
296 The epidermis flats were washed with PBS and fixed with cold acetone, then used for the following  
297 immunofluorescence staining like frozen sections.

298

299 Flow cytometry

300 The single-cell suspensions of mouse ears were prepared based on the method described previously<sup>58</sup>.  
301 <sup>59</sup>. Briefly, the ears were split and cut, incubated with a solution of RPMI containing 1mg/ml DNase I  
302 (NIPPON GENE, Tokyo, Japan) and 1mg/ml collagenase (Worthington Biochemical, Lakewood, NJ,  
303 USA) 90 min at 37 °C.  $1 \times 10^6$  cells of homogeneous cell suspension were stained with Alexa Fluor  
304 488 anti-mouse CD11c, Alexa Fluor 488 anti-mouse CD11b, PE anti-mouse CD115, PE anti-mouse

305 F4/80, PE anti-mouse I-A/I-E Alexa Fluor 647 anti-mouse CD206 according to the recommended  
306 concentration. Cells were analyzed on BD FACSVerse™ (BDBiosciences, San Jose, CA, USA).

307

### 308 Cell culture and siRNA transfection

309 Mouse keratinocyte cell line Pam2.12 was kindly provided by Dr. S. H. Yuspa (National Cancer  
310 Institute, Bethesda)<sup>60</sup>. The cells were cultured in DMEM (nacalai tesque, Kyoto, Japan) supplemented  
311 with 10% FBS and 1% penicillin/streptomycin/amphotericin B in a humidified atmosphere of 5% CO<sub>2</sub>  
312 at 37°C. Pam2.12 cells were stimulated with 250μM NiCl<sub>2</sub> for 0, 6, 12, 24, 48, 72 h before analysis  
313 (The concentration was decided according to previous study<sup>11</sup>). The Sema3A esiRNA was obtained  
314 from Sigma-Aldrich (Tokyo, Japan). Pam2.12 cells were transfected with 50nM of Sema3A siRNA  
315 using INTERFERin (Polyplus transfection, Illkirch, France) in half-decreased-volume serum free  
316 DMEM, after 4 h, complete DMEM was added to restore the usual culture volume. Medium was  
317 changed 24h after transfection and 250μM NiCl<sub>2</sub> was added to the cells for another 24 and 48 h.

318

### 319 Immunocytochemistry

320 Pam2.12 cells were seeded in dish with glass coverslips in the bottom. 300μM NiCl<sub>2</sub> was added

321 when cells grew to 40% confluency. After NiCl<sub>2</sub> stimulation for 24 or 48 h, coverslips were removed  
322 and washed with PBS, followed by fixation with 4% paraformaldehyde at room temperature for 10  
323 minutes. Then the coverslips were incubated in 0.25% Triton X-100 in PBS at room temperature for  
324 another 10 minutes and blocked in 3% BSA for 30 minutes. Finally, they were stained with  
325 immunofluorescence like frozen sections.

326

#### 327 Quantitative RT-PCR

328 The total RNA of Pam2.12 and the total RNA of mouse ears were extracted. cDNA was made using  
329 PrimeScript™ RT reagent Kit (TaKaRa Biotech, Shiga, Japan). TaKaRa Ex Taq® DNA Polymerase  
330 (TaKaRa Biotech, Shiga, Japan) was used for preliminary experiment to confirm expressions. qPCR  
331 was performed using TB Green® Premix Ex Taq™ II (TaKaRa Biotech, Shiga, Japan) in a total volume  
332 of 15µl with ABI7300 Real-time PCR System (Applied Biosystems, MA, USA) according to  
333 manufacturer instructions. The polymerase was initially activated at 95°C for 30 seconds, then the PCR  
334 was run in 40 cycles of denaturation at 95°C for 5 seconds and annealing/extension at 60°C for 31  
335 seconds. The sequences for primers were as follows: Sema3a, forward: 5'-  
336 GAAGAGCCCTTATGATCCCAAAC-3'; reverse: 5'-AGATAGCGAAGTCCCGTCCC-3'. Tnf-

337 alpha, forward: 5'-ATGGCCTCCCTCTCATCAGT-3'; reverse: 5'-CTTGGTGGTTTGCTACGACG-  
338 3'. Il1b, forward: 5'-GCTGAAAGCTCTCCACCTCA-3'; reverse: 5'-  
339 AGGCCACAGGTATTTTGTGCG-3'. Il17a, forward: 5'-GCTCCAGAAGGCCCTCAG-3'; reverse:  
340 5'-CTTCCCTCCGCATTGACA-3'. Il23, forward: 5'-CCAGCAGCTCTCTCGGAATC-3'; reverse:  
341 5'-TCATATGTCCCGCTGGTGC-3'. Cxcl1, forward: 5'-CCGAAGTCATAGCCACACTCAA-3';  
342 reverse: 5'-GCAGTCTGTCTTCTTTCTCCGTTA-3'. Ccl20, forward: 5'-  
343 GTACTGCTGGCTCACCTCTG-3'; reverse: 5'-CTTCATCGGCCATCTGTCTTGTG-3'. Actb,  
344 forward: 5'-TCTGGCTCCTAGCACCATGAAGA-3'; reverse: 5'-  
345 GGGACTCATCGTACTCCTGCTTG-3'. Gene expression was normalized to levels of  $\beta$ -actin.

346

347 Western blotting analysis

348 NiCl<sub>2</sub>-stimulated Pam2.12 cells were washed in cold PBS before lysis in 60 $\mu$ l of RIPA buffer  
349 (FUJIFILM Wako Pure Chemical Corporation, Osaka, Japan) containing 1:100 EZBlock™ Protease  
350 Inhibitor Cocktail (BioVision, San Francisco, CA, USA). Tissue extracts were prepared by  
351 homogenizing mouse ear tissue in lysis buffer. Proteins were separated in a 10% SDS-PAGE  
352 acrylamide gel for Pam2.12, transferred onto a polyvinylidene fluoride (PVDF) membrane.

353 Membranes were incubated with primary antibodies against Sema3A, TSLP, phosphorylated-p38  
354 MAPK at 4°C overnight. Total p38 MAPK and GAPDH were incubated at room temperature for 1 h.  
355 All the primary antibodies were used at a dilution 1:1000. After washing with TBST (0.05M Tris-HCl,  
356 0.15M NaCl, pH7.6), a 1:20000 dilution of HRP-conjugated anti-mouse secondary antibody was  
357 applied to the membrane for 1 h at room temperature. Membranes were detected with ECL Prime  
358 reagents (GE healthcare, Chicago, IL, USA) using ChemiDoc XRS (Bio-Rad, Hercules, CA, USA).

359

360 ELISA

361 Pam2.12 cells were seeded in 96-well dish and stimulated with 250µM NiCl<sub>2</sub> for 0, 12, 24, 48, 72 h  
362 before analysis of Sema3A production in medium using a mouse Sema3A ELISA kit (Signalway  
363 Antibody, College Park, MD, USA). Pam2.12 cells seeded in 96-well dish was performed with  
364 Sema3A siRNA transfection using INTERFERin as described above to suppress Sema3A expression.  
365 Culture supernatant 24 h after NiCl<sub>2</sub>-stimulation was collected and stored at -20°C until analysis. The  
366 TNF-α production was measured using a mouse TNF-α ELISA (eBioscience, San Diego, CA, USA),  
367 according to the manufacturer instructions.

368

369 **Statistical analysis**

370 All experiments were repeated at least three times with similar results. Experimental values are  
371 given as means  $\pm$  SD. The statistical difference was determined by One-Way ANOVA with LSD (Least  
372 Significant Difference), Tukey's HSD (honestly significant difference) test or Two independent  
373 samples t test. Statistical significance is presented in the following manner: \* $p < 0.05$ , \*\* $p < 0.01$ , \*\*\* $p$   
374  $< 0.001$ .

375

376 **Data availability**

377 The authors declare that the data supporting the findings of this study are available within the paper  
378 and from the authors upon reasonable requests. Source data are provided with this paper.

379

380 **References**

- 381 1. Lundström, I. M. Allergy and corrosion of dental materials in patients with oral lichen  
382 planus. *Int. J. Oral. Surg.* **13**, 16-24 (1984).

- 383 2. Scalf, L. A., Fowler Jr, J. F., Morgan, K. W. & Looney, S. W. Dental metal allergy in patients  
384 with oral, cutaneous, and genital lichenoid reactions. *Am. J. Contact Dermat.* **12**, 146-150  
385 (2001).
- 386 3. Mizoguchi, S., Setoyama, M. & Kanzaki, T. Linear lichen planus in the region of the mandibular  
387 nerve caused by an allergy to palladium in dental metals. *Dermatology.* **196**, 268-70 (1998).
- 388 4. Laine, J., Kalimo, K. & Happonen, R. P. Contact allergy to dental restorative materials in  
389 patients with oral lichenoid lesions. *Contact Dermatitis.* **36**, 141-146 (1997).
- 390 5. Song, H., Yin, W. & Ma, Q. Allergic palmoplantar pustulosis caused by cobalt in cast dental  
391 crowns:a case report. *Oral Surg. Oral Med. Oral Pathol. Oral Radiol. Endod.* **111**, e8-e10  
392 (2011).
- 393 6. Wataha, J. C. & Khajotia, S. S. Effect of pH on element release from dental casting alloys. *J.*  
394 *Prosthet. Dent.* **80**, 691-698(1998).
- 395 7. Saito, M. et al. Molecular mechanisms of nickel allergy. *Int. J. Mol. Sci.* **17**, 202 (2016).
- 396 8. Tu, M. E. & Wu, Y. H. Multiple allergies to metal alloys. *Dermatologica Sinica.* **29**, 41-43  
397 (2011).

- 398 9. Watanabe, M. et al. A novel DC therapy with manipulation of MKK6 gene on nickel allergy in  
399 mice. *PLoS One*. **6**, e19017 (2011).
- 400 10. Ashrin, M. N. et al. A critical role for thymic stromal lymphopoietin in nickel-induced allergy in  
401 mice. *J. Immunol.* **192**, 4025-4031 (2014).
- 402 11. Minami, N., Watanabe, M., Liu, L., Yunizar, M. F. & Ichikawa, T. Effect of Semaphorin7A  
403 during the Effector Phase of Nickel Allergy. *Journal of Oral Health and Biosciences*. **33**, 8-14  
404 (2020).
- 405 12. Fujisawa, H. Discovery of semaphorin receptors, neuropilin and plexin, and their functions in  
406 neural development. *J. Neurobiol.* **59**, 24-33 (2004).
- 407 13. Toledano, S., Nir-Zvi, I., Engelman, R., Kessler, O. & Neufeld, G. Class-3 semaphorins and  
408 their receptors: potent multifunctional modulators of tumor progression. *Int. J. Mol. Sci.* **20**, 556  
409 (2019).
- 410 14. Ji, J. D., Park-Min, K. H. & Ivashkiv, L. B. Expression and function of semaphorin 3A and its  
411 receptors in human monocyte-derived macrophages. *Hum. Immunol.* **70**, 211-217 (2009).
- 412 15. Catalano, A. et al. Semaphorin-3A is expressed by tumor cells and alters T-cell signal  
413 transduction and function. *Blood*. **107**, 3321-3329 (2006).

- 414 16. Yamamoto, M. et al. Plexin-A4 negatively regulates T lymphocyte responses. *Int. Immunol.* **20**,  
415 413-420 (2008).
- 416 17. Takamatsu, H. et al. Semaphorins guide the entry of dendritic cells into the lymphatics by  
417 activating myosin II. *Nat. Immunol.* **11**, 594-600 (2010).
- 418 18. Yamashita, N. et al. Anti-Semaphorin 3A neutralization monoclonal antibody prevents sepsis  
419 development in lipopolysaccharide-treated mice. *Int. Immunol.* **27**, 459-466 (2015).
- 420 19. Garcia, S. Role of semaphorins in immunopathologies and rheumatic diseases. *Int. J. Mol.*  
421 *Sci.* **20**, 374 (2019).
- 422 20. Tanaka, J. et al. Semaphorin 3A controls allergic and inflammatory responses in experimental  
423 allergic conjunctivitis. *Int. J. Ophthalmol.* **8**, 1 (2015).
- 424 21. Xiang, R. et al. Semaphorin 3A inhibits allergic inflammation by regulating immune responses  
425 in a mouse model of allergic rhinitis. *Int. Forum Allergy Rhinol.* **9**, 528-537 (2019).
- 426 22. Yamaguchi, J. et al. Semaphorin3A alleviates skin lesions and scratching behavior in NC/Nga  
427 mice, an atopic dermatitis model. *J. Invest. Dermatol.* **128**, 2842-2849 (2008).

- 428 23. Negi, O. et al. Topically applied semaphorin 3A ointment inhibits scratching behavior and  
429 improves skin inflammation in NC/Nga mice with atopic dermatitis. *J. Dermatol. Sci.* **66**, 37-43  
430 (2012).
- 431 24. Tominaga, M. & Takamori, K. Itch and nerve fibers with special reference to atopic  
432 dermatitis:therapeutic implications. *J. Dermatol.* **41**, 205-212 (2014).
- 433 25. Nguyen, A. V. & Soulika, A. M. The dynamics of the skin's immune system. *Int. J. Mol. Sci.* **20**,  
434 1811 (2019).
- 435 26. Liu, Y. J. Thymic stromal lymphopoietin:master switch for allergic inflammation. *J. Exp.*  
436 *Med.* **203**, 269-273 (2006).
- 437 27. Kamata, Y. et al. Calcium-Inducible MAPK/AP-1 Signaling Drives Semaphorin 3A Expression  
438 in Normal Human Epidermal Keratinocytes. *J. Invest. Dermatol.* **140**, 1346-1354 (2020).
- 439 28. Tominaga, M., Ogawa, H. & Takamori, K. Decreased production of semaphorin 3A in the  
440 lesional skin of atopic dermatitis. *Br. J. Dermatol.* **158**, 842-844 (2008).
- 441 29. Tominaga, M., Tenggara, S., Kamo, A., Ogawa, H. & Takamori, K. Psoralen-ultraviolet A  
442 therapy alters epidermal Sema3A and NGF levels and modulates epidermal innervation in atopic  
443 dermatitis. *J. Dermatol. Sci.* **55**, 40-46 (2009).

- 444 30. Ikezawa, Z. et al. A role of Staphyococcus aureus, interleukin-18, nerve growth factor and  
445 semaphorin 3A, an axon guidance molecule, in pathogenesis and treatment of atopic  
446 dermatitis. *Allergy Asthma Immunol. Res.* **2**, 235 (2010).
- 447 31. Tang, X. Q., Tanelian, D. L. & Smith, G. M. Semaphorin3A inhibits nerve growth factor-  
448 induced sprouting of nociceptive afferents in adult rat spinal cord. *J. Neurosci.* **24**, 819-827  
449 (2004).
- 450 32. Zhang, M. et al. Semaphorin3A induces nerve regeneration in the adult cornea-a switch from its  
451 repulsive role in development. *PloS one.* **13**, e0191962 (2018).
- 452 33. Gragnani, A. et al. Gene expression profile of cytokines and receptors of inflammation from  
453 cultured keratinocytes of burned patients. *Burns.* **40**, 947-956 (2014).
- 454 34. Guilloteau, K. et al. Skin inflammation induced by the synergistic action of IL-17A, IL-22,  
455 oncostatin M, IL-1 $\alpha$ , and TNF- $\alpha$  recapitulates some features of psoriasis. *J. Immunol.* **184**, 5263-  
456 5270 (2010).
- 457 35. Milward, M. R. et al. Differential activation of NF- $\kappa$ B and gene expression in oral epithelial  
458 cells by periodontal pathogens. *Clin. Exp. Immunol.* **148**, 307-324 (2007).

- 459 36. Ito, T., Morita, T., Yoshida, K., Negishi, T. & Yukawa, K. Semaphorin 3A-Plexin-A1 signaling  
460 through ERK activation is crucial for Toll-like receptor-induced NO production in BV-2  
461 microglial cells. *Int. J. Mol. Med.* **33**, 1635-1642 (2014).
- 462 37. Ito, T. et al. Plexin-A1 is required for Toll-like receptor-mediated microglial activation in the  
463 development of lipopolysaccharide-induced encephalopathy. *Int. J. Mol. Med.* **33**, 1122-1130  
464 (2014).
- 465 38. Lee, J. C. et al. A protein kinase involved in the regulation of inflammatory cytokine  
466 biosynthesis. *Nature*, **372**, 739-746 (1994).
- 467 39. Canovas, B. & Nebreda, A. R. Diversity and versatility of p38 kinase signalling in health and  
468 disease. *Nat Rev Mol Cell Biol*, **22**, 346-366 (2021).
- 469 40. Theivanthiran, B. et al. The E3 ubiquitin ligase Itch inhibits p38 $\alpha$  signaling and skin  
470 inflammation through the ubiquitylation of Tab1. *Sci Signal*, **8**, ra22-ra22 (2015).
- 471 41. Marble, D. J., Gordon, K. B. & Nickoloff, B. J. Targeting TNF $\alpha$  rapidly reduces density of  
472 dendritic cells and macrophages in psoriatic plaques with restoration of epidermal keratinocyte  
473 differentiation. *J. Dermatol. Sci.* **48**, 87-101 (2007).

- 474 42. Nosenko, M. A., Ambaryan, S. G. & Drutskaya, M. S.. Proinflammatory cytokines and skin  
475 wound healing in mice. *Mol. Biol. (Mosk)*. **53**, 653-664 (2019).
- 476 43. Banno, T., Gazel, A. & Blumenberg, M. Effects of tumor necrosis factor- $\alpha$  (TNF $\alpha$ ) in epidermal  
477 keratinocytes revealed using global transcriptional profiling. *J. Biol. Chem.* **279**, 32633-32642  
478 (2004).
- 479 44. Silva, R. L., Lopes, A. H., Guimarães, R. M. & Cunha, T. M. CXCL1/CXCR2 signaling in  
480 pathological pain: role in peripheral and central sensitization. *Neurobiol Dis*, **105**, 109-  
481 116(2017).
- 482 45. Abumaree, M. H. et al. Human placental mesenchymal stem cells (pMSCs) play a role as  
483 immune suppressive cells by shifting macrophage differentiation from inflammatory M1 to anti-  
484 inflammatory M2 macrophages. *Stem Cell Rev. Rep.* **9**, 620-641 (2013).
- 485 46. Van Dalen, F. J., Van Stevendaal, M. H., Fennemann, F. L., Verdoes, M. & IJina, Q. Molecular  
486 repolarisation of tumour-associated macrophages. *Molecules*. **24**, 9 (2019).
- 487 47. Wang, L. X., Zhang, S. X., Wu, H. J., Rong, X. L. & Guo, J. M2b macrophage polarization and  
488 its roles in diseases. *J. Leukoc. Biol.* **106**, 345-358 (2019).

- 489 48. Kratochvill, F. et al. TNF counterbalances the emergence of M2 tumor macrophages. *Cell*  
490 *Rep.* **12**, 1902-1914 (2015).
- 491 49. Batra, R. et al. IL-1 $\beta$  (interleukin-1 $\beta$ ) and TNF- $\alpha$  (tumor necrosis factor- $\alpha$ ) impact abdominal  
492 aortic aneurysm formation by differential effects on macrophage polarization. *Arterioscler.*  
493 *Thromb. Vasc. Biol.* **38**, 457-463 (2018).
- 494 50. Rienks, M. et al. Sema3A promotes the resolution of cardiac inflammation after myocardial  
495 infarction. *Basic Res. Cardiol.* **112**, 1-13 (2017).
- 496 51. Murota, H., Abd El-latif, M., Tamura, T., Amano, T. & Katayama, I. Olopatadine hydrochloride  
497 improves dermatitis score and inhibits scratch behavior in NC/Nga mice. *Int. Arch. Allergy*  
498 *Immunol.* **153**, 121-132 (2010).
- 499 52. Tominaga, M. & K. Takamori. Recent advances in pathophysiological mechanisms of  
500 itch. *Expert. Rev. Dermatol.* **5**, 197-212 (2010).
- 501 53. Tarutani, M. et al. Tissue-specific knockout of the mouse Pig-a gene reveals important roles for  
502 GPI-anchored proteins in skin development. *Proc. Natl. Acad. Sci.* **94**, 7400-7405(1997).
- 503 54. Moullan, N. Rapid and effective genotyping of Cre transgenic mice. *Application Guide*, **19**  
504 (2016).

- 505 55. Taniguchi, M. et al. Disruption of semaphorin III/D gene causes severe abnormality in  
506 peripheral nerve projection. *Neuron*. **19**, 519-530 (1997).
- 507 56. Tschachler, E. et al. Expression of Thy-1 antigen by murine epidermal cells. *J. Invest.*  
508 *Dermatol.* **81**, 282-285 (1983).
- 509 57. Jameson, J. et al. A role for skin  $\gamma\delta$  T cells in wound repair. *Science*. **296**, 747-749 (2002).
- 510 58. Ober-Blöbaum, J. L. et al. Monitoring skin dendritic cells in steady state and inflammation by  
511 immunofluorescence microscopy and flow cytometry. *Methods Mol. Biol.* **1559**, 37-52 (2017).
- 512 59. Broggi, A., Cigni, C., Zanoni, I. & Granucci, F. Preparation of single-cell suspensions for  
513 cytofluorimetric analysis from different mouse skin regions. *J. Vis. Exp.* **110**, e52589 (2016).
- 514 60. Yuspa, S. H., Hawley-Nelson, P., Koehler, B. & Stanley, J. R. A survey of transformation  
515 markers in differentiating epidermal cell lines in culture. *Cancer Res.* **40**, 4694-4703 (1980).

516

## 517 **Competing Interests**

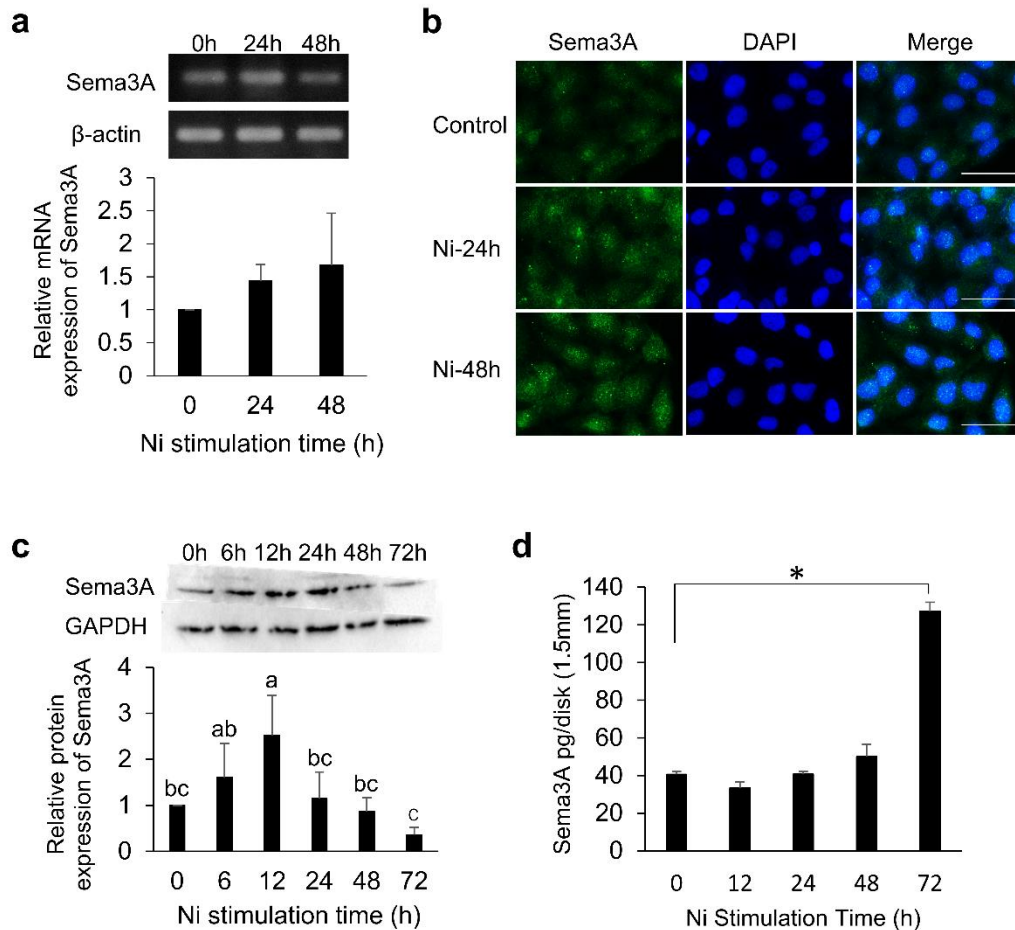
518 Disclosures: The authors declare no competing interests exist.

519

520

521 **Figures**

522 **Figure 1. Sema3A expression.**



523

524 **a** Sma3A was expressed on NiCl<sub>2</sub>-stimulated Pam2.12 and the mRNA expression increased after NiCl<sub>2</sub>

525 stimulation. **b** Immunocytochemistry of Sema3A expressed in Pam2.12 24 h and 48 h after NiCl<sub>2</sub>

526 stimulation. Scale bar, 50µm. **c** Upregulated Sema3A in NiCl<sub>2</sub>-stimulated Pam2.12 was analyzed by

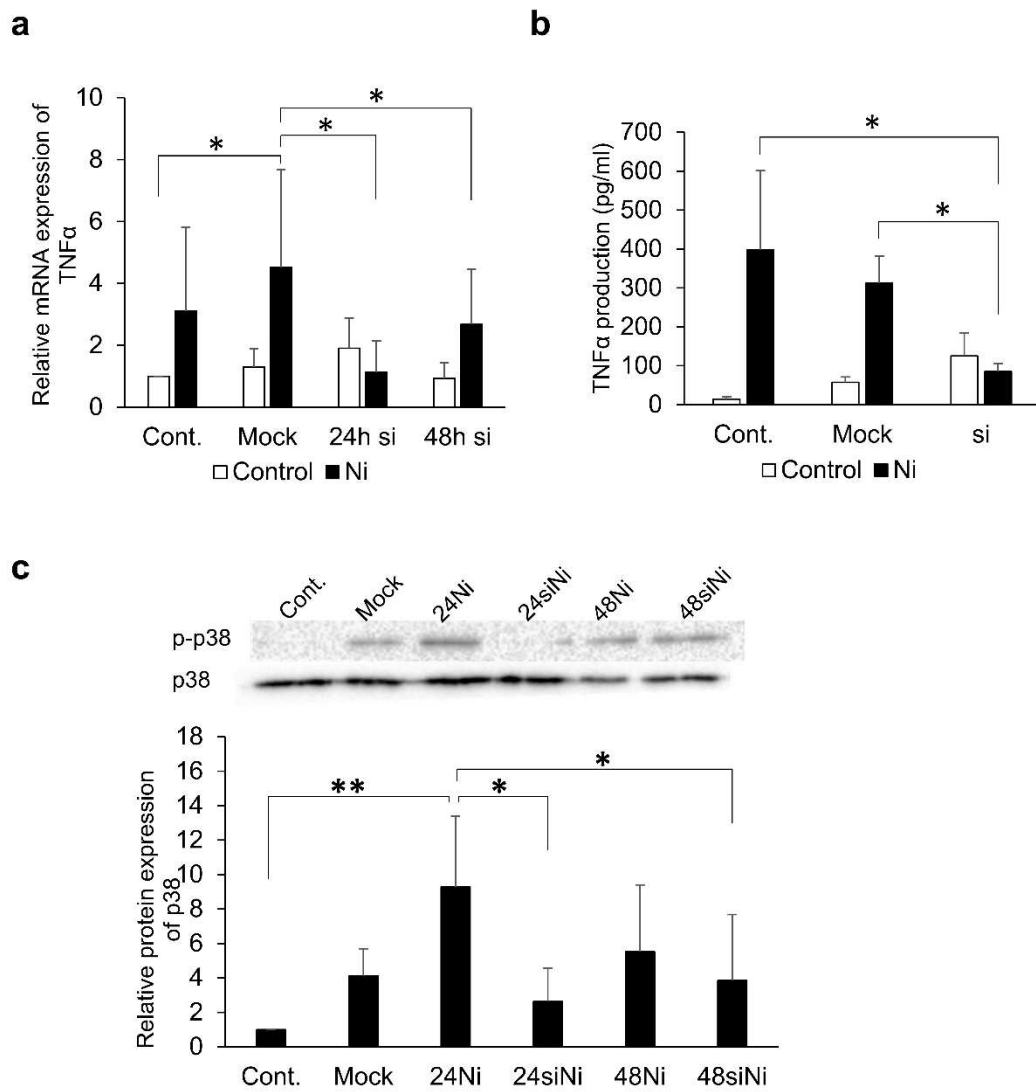
527 Western blotting analysis. GAPDH was used as the internal control. **d** Upregulated Sema3A production

528 in NiCl<sub>2</sub>-stimulated Pam2.12 was analyzed by ELISA. Data are shown as mean ± SD and are

529 representative of at least three independent experiments. Different letters on bars indicate significant  
 530 differences. \* $p < 0.05$ ; One-Way ANOVA with LSD. Source data and p values are provided as a Source  
 531 Data file.

532

533 **Figure 2. Effect of Sema3A siRNA.**



534

535 **a** TNF $\alpha$  mRNA expression in Sema3A siRNA-treated Pam2.12 after NiCl<sub>2</sub> stimulation was analyzed  
536 using quantitative RT-PCR. Gene expression was normalized to levels of  $\beta$ -actin. 24h si/48h si  
537 represents Sema3A siRNA-treated groups with or without 24/48 h-NiCl<sub>2</sub> stimulation. **b** TNF $\alpha$  protein  
538 production in Sema3A siRNA-treated Pam2.12 after NiCl<sub>2</sub> stimulation was analyzed by ELISA. The  
539 samples with or without NiCl<sub>2</sub> stimulation were collected after 24 h. **c** Inhibited p38 phosphorylation  
540 in Sema3A siRNA-treated Pam2.12 after NiCl<sub>2</sub> stimulation was analyzed by Western blotting analysis.  
541 GAPDH was used as the internal control. 24Ni/48Ni represents the groups with 24/48 h-NiCl<sub>2</sub>  
542 stimulation. 24siNi/48siNi represents the Sema3A siRNA-treated groups with 24/48 h-NiCl<sub>2</sub>  
543 stimulation. Data are shown as mean  $\pm$  SD and are representative of at least three independent  
544 experiments. \*p<0.05, \*\*p<0.01; One-Way ANOVA with LSD. Source data and p values are provided  
545 as a Source Data file.

546

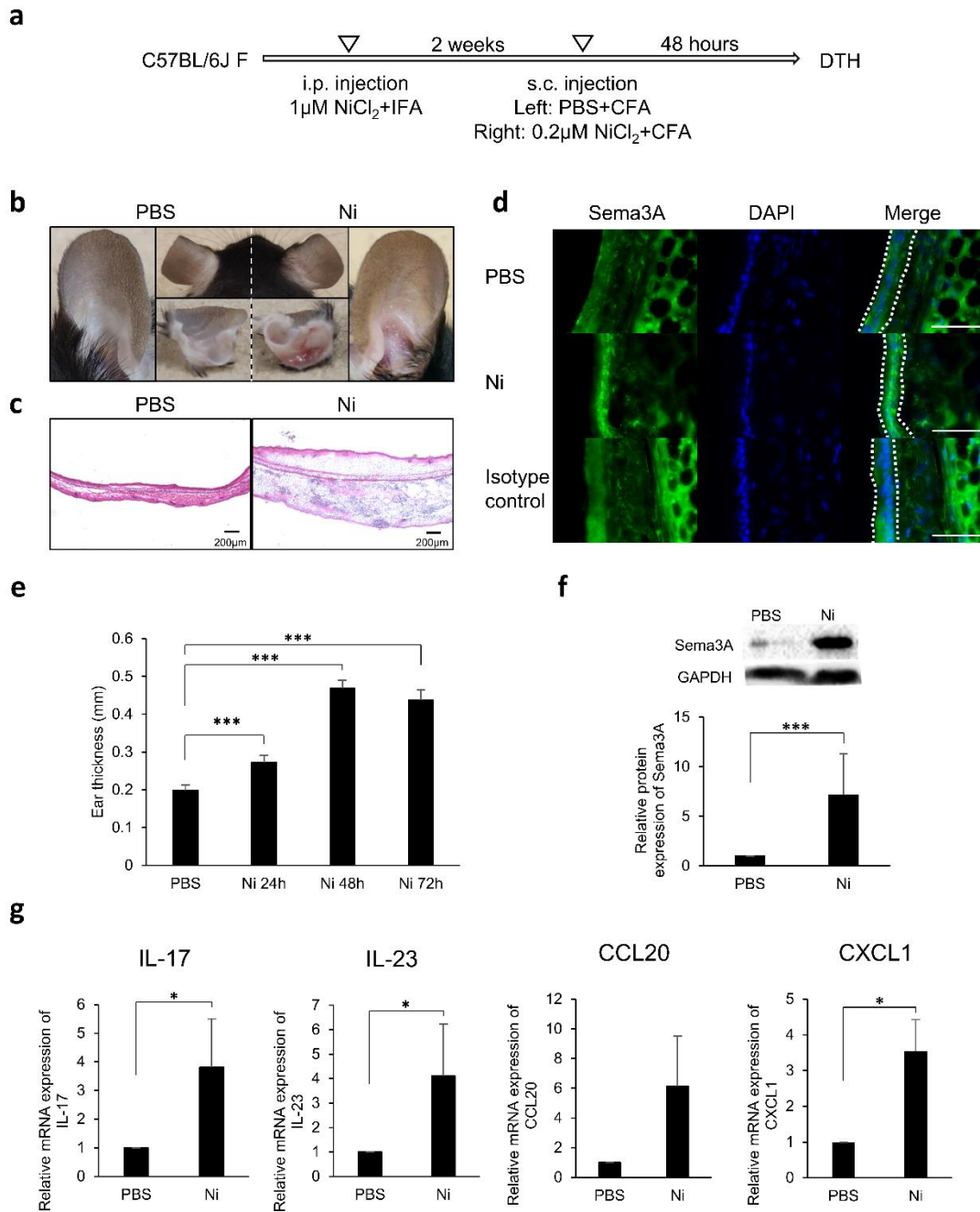
547

548

549

550

551 **Figure 3. Sema3A and cytokine/chemokine expression in allergy site.**



552

553 **a** Protocol for inducing Ni allergy in mouse ear tissue. **b** Representative photos of the Ni allergy-

554 induced mouse ear and the control ear. Photos show the ventral side (right and left), dorsal side (middle

555 upper) and cross-section (middle lower). **c** Histological images of Ni allergy-induced mouse ear tissue

556 and control ear tissue. Scale bar, 200 $\mu$ m. **d** Sema3A expression in the control and Ni allergy-induced  
557 ear tissue was stained using immunofluorescence assays. Staining without Anti-rabbit Fluor Alexa 488  
558 secondary antibody was set for isotype control. Dashed line shows the epidermis zone. Scale bar, 50 $\mu$ m.  
559 **e** DTH was determined by ear thickness measuring after Ni re-challenge. Data are shown as mean  $\pm$   
560 SD of 5 mice/group. **f** Upregulated Sema3A expression in Ni allergy-induced mouse ear tissue was  
561 analyzed by Western blotting analysis. GAPDH was used as the internal control. **g** The mRNA  
562 expression of inflammatory cytokine/chemokine in Ni allergy-induced mouse ear tissue were analyzed  
563 using quantitative RT-PCR. Gene expression was normalized to levels of  $\beta$ -actin. Data are shown as  
564 mean  $\pm$  SD and are representative of at least three independent experiments. \* $p$ <0.05, \*\*\* $p$ <0.001;  
565 Tukey's test for **e** and Two independent samples t test for **f** and **g**. Source data and  $p$  values are provided  
566 as a Source Data file.

567

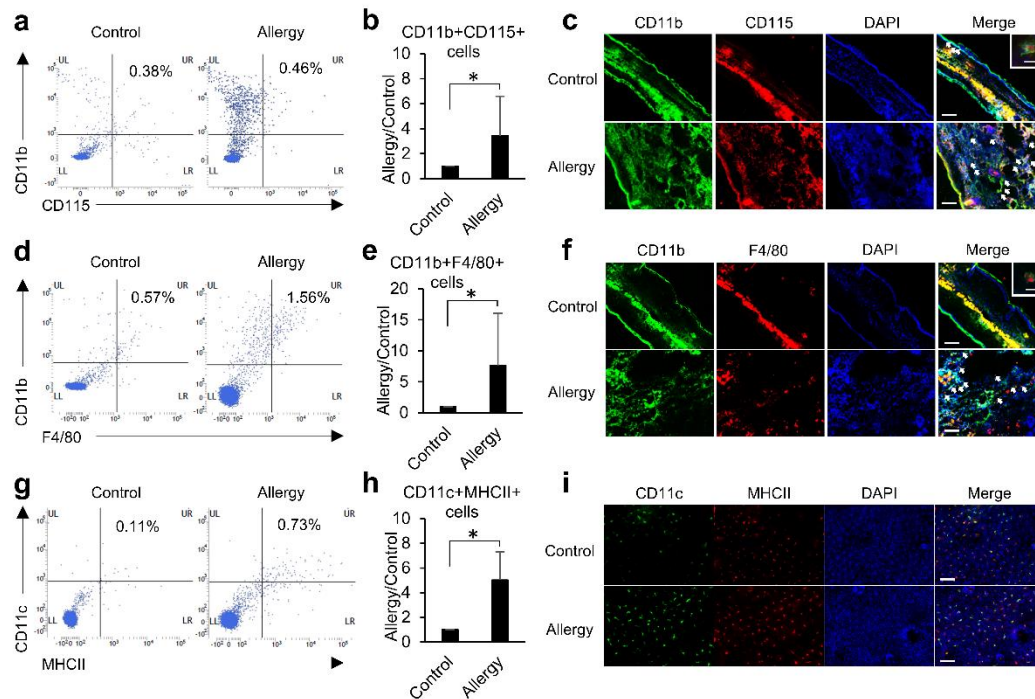
568

569

570

571

572 **Figure 4. Cell population in allergy site.**



573

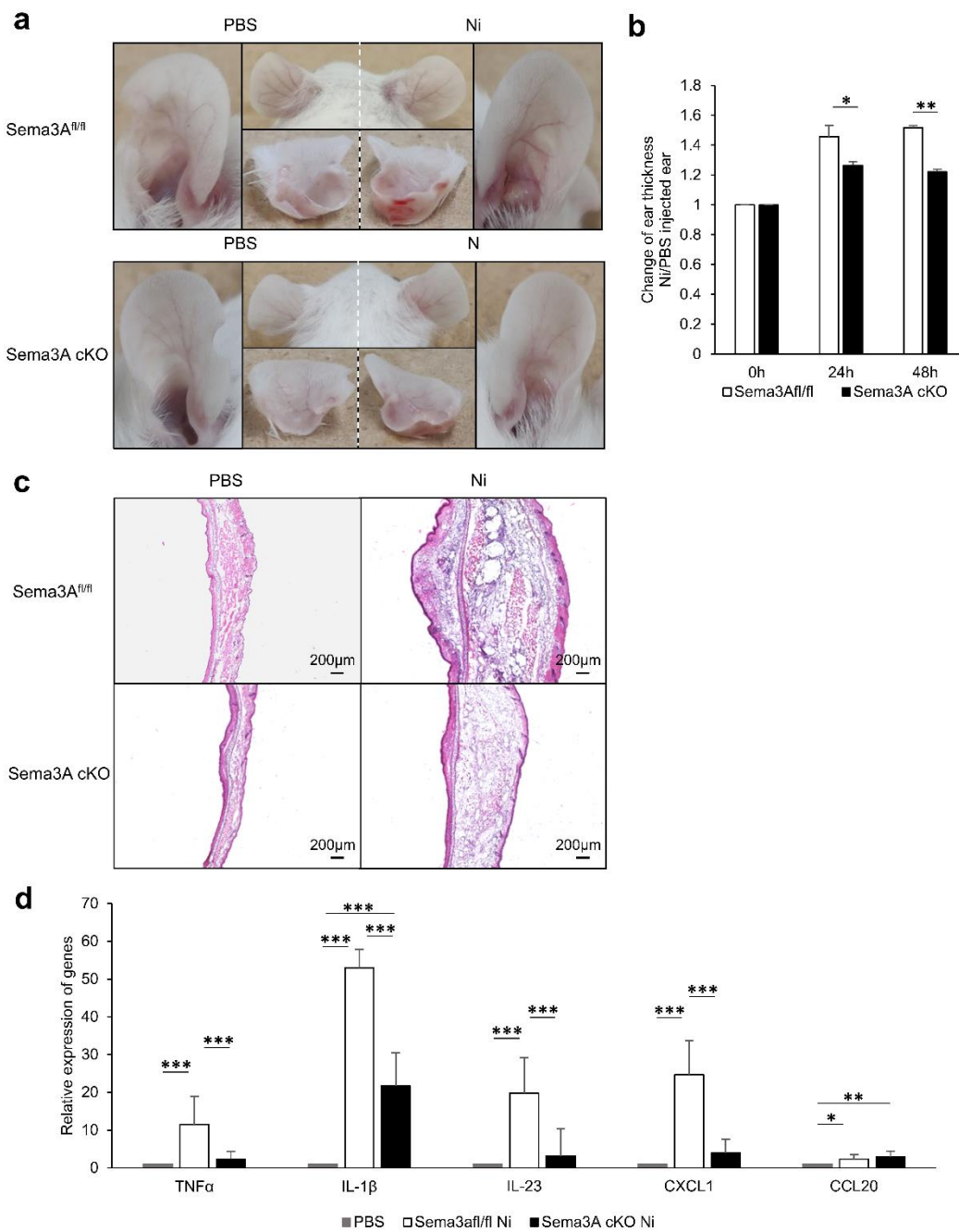
574 **a, d, g** The population of CD11b<sup>+</sup>CD115<sup>+</sup> monocytes (**a**), CD11b<sup>+</sup>F4/80<sup>+</sup> macrophages (**d**), and  
 575 CD11c<sup>+</sup>MHCII<sup>+</sup> DCs (**g**) in mouse ear tissue was analyzed by flow cytometry. **b, e, h** The number of  
 576 CD11b<sup>+</sup>CD115<sup>+</sup> monocytes (**b**), CD11b<sup>+</sup>F4/80<sup>+</sup> macrophages (**e**), and CD11c<sup>+</sup>MHCII<sup>+</sup> DCs (**h**) in the  
 577 Ni allergy-induced mouse ear tissue was increased. Data are shown as mean ± SD of 3 mice/group and  
 578 are representative of four independent experiments. **c, f** CD11b<sup>+</sup>CD115<sup>+</sup> monocytes (**c**) and  
 579 CD11b<sup>+</sup>F4/80<sup>+</sup> macrophages (**f**) in the control and Ni allergy-induced ear tissue were stained using  
 580 immunofluorescence assays. Arrows indicate double-positive cell location. Scale bar, 100µm. Higher  
 581 magnification images of CD11b<sup>+</sup>CD115<sup>+</sup> monocyte and CD11b<sup>+</sup>F4/80<sup>+</sup> macrophage are shown in the  
 582 upper right of the control group images. Scale bar, 10µm. **i** CD11c<sup>+</sup>MHCII<sup>+</sup> DCs in the epidermal sheet

583 of mouse ears were analyzed using immunofluorescence assays. Scale bar, 100 $\mu$ m. \* $p$ <0.05. Two

584 independent samples t test. Source data and p values are provided as a Source Data file.

585

586 **Figure 5. Allergy symptoms in Sema3A cKO mouse.**



587

588 **a** Representative photos of the Ni allergy-induced ear and control ear of Sema3A<sup>fl/fl</sup> and Sema3A cKO  
589 groups. Photos show the ventral side (right and left), dorsal side (middle upper) and cross-section  
590 (middle lower). **b** DTH was determined by ear thickness measuring after Ni re-challenge. The ratio of  
591 allergy/control ear thickness of Sema3A<sup>fl/fl</sup> and Sema3A cKO mice is shown to present the change of  
592 ear thickness. Data are shown as mean  $\pm$  SD of 3 mice/group. **c** Histological images of the Ni allergy-  
593 induced mouse ear tissue and control ear tissue of Sema3A<sup>fl/fl</sup> and Sema3A cKO groups. Scale bar,  
594 200 $\mu$ m. **d** The mRNA expressions of related cytokines/chemokines in Ni allergy-induced mouse ear  
595 tissue of Sema3A<sup>fl/fl</sup> and Sema3A cKO groups were analyzed using quantitative RT-PCR. Gene  
596 expression was normalized to levels of  $\beta$ -actin. \* $p$ <0.05, \*\* $p$ <0.01, \*\*\* $p$ <0.001. Two independent  
597 samples t test for **b**, and One-Way ANOVA with LSD for **d**. Source data and p values are provided as  
598 a Source Data file.

599

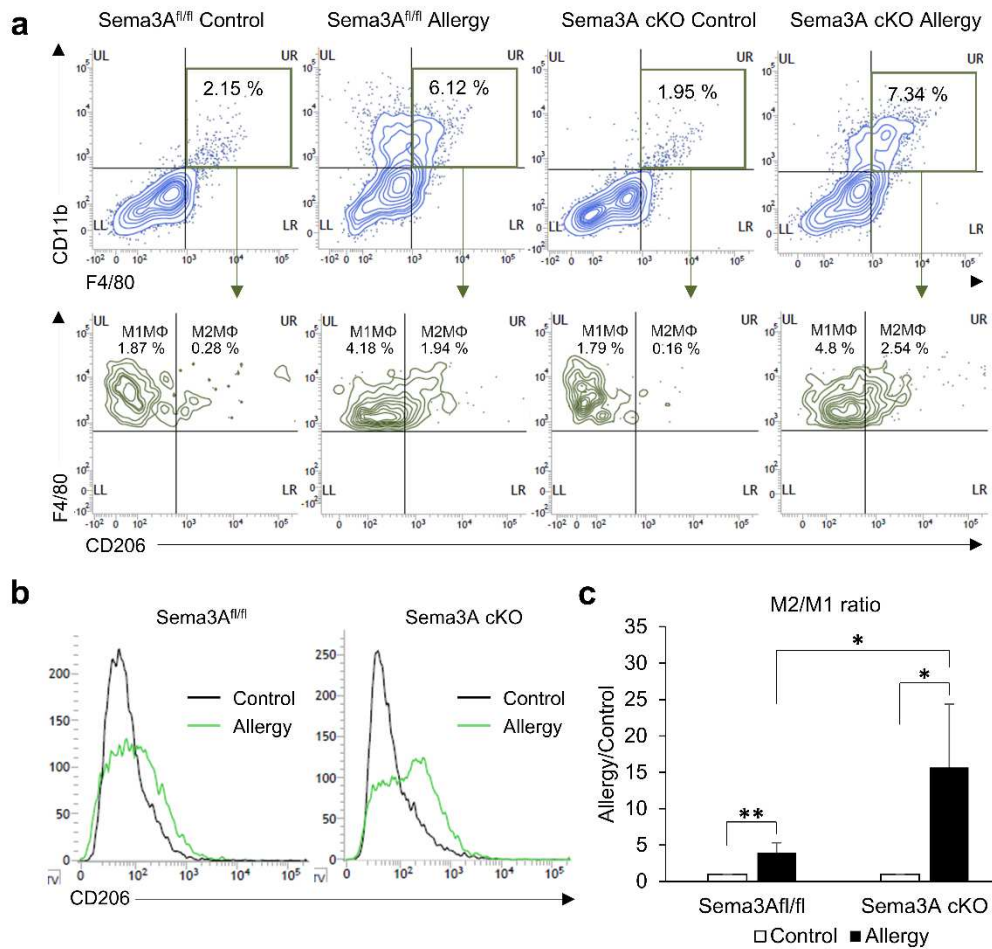
600

601

602

603

604 **Figure 6. Cell population in allergy site in cKO mouse.**



605

606 **a** The population of CD11b<sup>+</sup>F4/80<sup>+</sup> macrophages in Sema3A<sup>fl/fl</sup> and Sema3A cKO mouse ears was

607 analyzed by flow cytometry. MΦ represents for macrophage. M1-like MΦ was defined as CD206<sup>-</sup>

608 CD11b<sup>+</sup>F4/80<sup>+</sup> cells and M2-like MΦ was defined as CD206<sup>+</sup>CD11b<sup>+</sup>F4/80<sup>+</sup> cells. **b** Representative

609 flow cytometry analysis of CD206<sup>+</sup> cells in Sema3A<sup>fl/fl</sup> and Sema3A cKO mouse ears. Black lines

610 represent the control groups and green lines represent the Ni allergy groups. **c** M2/M1 ratio was

611 increased in Ni allergy-induced Sema3A cKO mouse ear compared to that in Sema3A<sup>fl/fl</sup> mice. Data

612 are shown as mean  $\pm$  SD and are representative of four independent experiments. \*p<0.05, \*\*p<0.01.  
613 Two independent samples t test and One-Way ANOVA with LSD. Source data and p values are  
614 provided as a Source Data file.

## Supplementary Files

This is a list of supplementary files associated with this preprint. Click to download.

- [SupplementaryInformation.pdf](#)
- [SourceData.xlsx](#)
- [ReportingSummary.pdf](#)
- [rs.pdf](#)